

Constant Power Operation Control of Variable Speed Wind Turbine DFIG using Genetic Algorithm

Gaber EL-Saady Ahmed, EL-Noby Ahmed Ibrahim and Hazem Hassan Ali

Electrical Engineering Department & Assiut University
Assiut, Egypt

Abstract - This paper presents a design of pitch controller using Genetic Algorithm (GA) for variable speed wind turbine Doubly Fed Induction Generator (DFIG). The proposed genetic pitch controller is used to get the proper pitch angle for limiting the mechanical power when the wind speed is greater than the rated wind speed. DFIG is a wound-rotor induction generator where the stator terminals of DFIG are connected directly to the grid and the rotor terminals of DFIG are connected to the mains via a partially rated variable frequency ac/dc/ac converter. The ac/dc/ac converter system consists of a rotor side converter (RSC) and a grid side converter (GSC) connected back-to-back by a DC-link capacitor. The stator voltage orientation (SVO) control algorithm is utilized for RSC which is controlled by hysteresis current controller. While the GSC is controlled by pulse width modulation (PWM). Due to the nature of unpredicted wind speed, determining the right value of pitch angle of wind turbine to limit the mechanical power at any wind speed above the rated wind speed is essential. By controlling the pitch angle of the wind turbine blades, the rotational speed and the output power are regulated at constant value. The system under study is simulated using MATLAB/Simulink package. The digital simulation results under different conditions in terms of the variations of the wind turbine generator show that the output power, rotor speed and torque responses for step change in wind speed prove the effectiveness and powerful of the proposed GA controller for pitch control.

Keywords – DFIG, Pitch Angle, Genetic Algorithm, Wind Turbine Control.

I. INTRODUCTION

In recent years more attention has been given to induction machines because they are used for low and medium power application. Attractive advantages over conventional generators are lower unit cost, less maintenance and robust construction etc. Doubly-Fed Induction Generators (DFIG) is particularly suitable for isolated operation like hydro and wind developments [1]. Doubly fed induction generators (DFIGs) are currently dominating the renewable energy market. Over the last decades, DFIG-based wind turbines have been most preferred option for the

high capacity wind farms because it has the ability to control the active and reactive power exchange within the network. DFIGs have the capability to operate in variable speed regions so we have to achieve a smoothed and twice the power than any other conventional generator will produce. In the development of wind turbine techniques, DFIG is becoming more popular because of its unique characteristics such as high efficiency, low cost and flexible control [2]. Doubly fed induction machines inherit all the advantages of a cage induction generator but the fact due to which they are more popular are that the stator of the DFIG is connected directly to the grid and it supplies power from the stator side at grid voltage and frequency. Other than that the control is done from the rotor side. So the power converters used for DFIG control are of less power rating, which reduces the cost as well as the switching losses, which results in enhanced efficiency. There are usually two modes for the DFIG variable-speed wind turbines which are cross coupled each other. The first mode, in low wind speed below rated value, the speed controller can continuously adjust the speed of the rotor to maintain the tip speed ratio constant at the level which gives the maximum power coefficient and then the efficiency of the turbine will be significantly increased, the generator is controlled by power electronic equipment, which makes it possible to control the rotor speed. The second mode, in high wind speed above rated value, pitch angle regulation is necessary in conditions above the rated wind speed where the rotational speed is kept constant. With every change in wind speed above rated wind speed, the value of pitch angle will be changed but the mechanical power is limited at its rated, the next sections will explain this concept. The purpose of the pitch angle was presented and studied [2-4]. The control systems for DFIG variable speed wind turbines prove on good performance as shown in the next sections.

II. WIND TURBINE DESCRIPTION

A. Operating Region of the Wind Turbine

The wind turbine operates, with different dynamics, from the cut-in wind speed (usually 4 m/s, for modern wind turbines) to the cut-out wind speed (around 24

m/s), as shown in Fig. 1. Three distinct wind speed points can be noticed in this power curve [5]:

- 1) V_{wind_cut-in} : The lowest wind speed at which wind turbine starts to generate power.
- 2) Rated wind speed: Wind speed at which the wind turbine generates the rated power, which is usually the maximum power wind turbine can produce.
- 3) $V_{wind_cut-out}$: Wind speed at which the turbine ceases power generation and is shut down (with automatic brakes and/or blade pitching) to protect the turbine from mechanical damage.

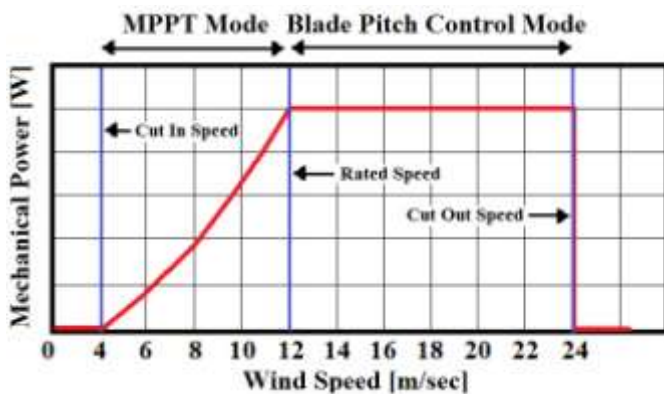


Fig. 1 Output power wind speed characteristic.

B. Aerodynamic of the Wind Turbine

The energy conversion in a wind turbine can be described by the nonlinear equations [6]:

$$P_{m} = 0.5\rho A V_w^3 C_p \tag{1}$$

Where P_m is the mechanical power (watt), ρ is the air density (kg/m^3), $A = \pi R^2$ is area covered by turbine blades (m^2), R is Rotor radius (m), V_w (m/sec) is the wind velocity and C_p is the coefficient of power. The maximum theoretical value of C_p is approximately 0.59 [7]. The power captured by the wind turbine depends highly on C_p for a given wind speed and the relationship of C_p with λ and β represents the output characteristics of the wind turbine as in (2):

$$C_p(\lambda, \beta) = 0.5176 \left(\frac{116}{\lambda_i} - 0.4\beta - 5 \right) e^{-\frac{21}{\lambda_i}} + 0.0068\lambda \tag{2}$$

Where λ is tip speed ratio (TSR), a variable expressing the linear speeds of blade tip to speed of wind turbine and β is the pitch angle, λ and $\frac{1}{\lambda_i}$ can be expressed as in (3) and (4), respectively.

$$\lambda = \frac{w_t R}{V_w} \tag{3}$$

Where w_t is rotational turbine speed (rad/sec).

$$\frac{1}{\lambda_i} = \frac{1}{\lambda + 0.08\beta} - \frac{0.035}{\beta^3 + 1} \tag{4}$$

By using (2), the typical C_p versus λ curve is shown in Fig. 2. This figure shows the power coefficient C_p as a function of λ at different values of pitch angle β . When the value of pitch angle increases, the value of maximum power coefficient will decrease. For β equal to zero this is the mode of maximum power point tracking mode where the optimum value of TSR will lead to maximum power coefficient but for values of pitch angle greater than zero this is for pitch control mode.

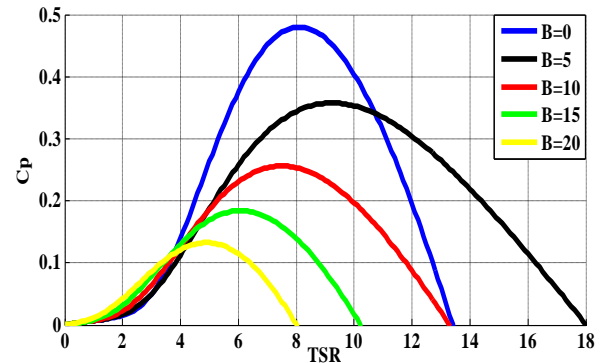


Fig. 2 Power coefficient $C_p(\lambda, \beta)$ versus λ for various values of pitch angle β .

The mode of pitch control mode is between the rated wind speed and cut out speed. When the wind speed increases beyond the rated value, the electromagnetic torque is not sufficient to control rotor speed because this leads to an overload on the generator and the converter. To prevent rotor speed from becoming too high, the extracted power from incoming wind must be limited. This can be done by reducing the coefficient of performance of the turbine (The C_p value). As explained earlier, the C_p value can be manipulated by changing the pitch angle as shown in Fig. 2. The wind speed is varied above rated wind speed, turbine speed is maintained at rated speed ($w_t = w_{t-rated}$) and the corresponding λ is calculated using (5):

$$\lambda = \frac{w_{t-rated} R}{V_w} \tag{5}$$

The C_p corresponding to rated power is calculated using (6):

$$C_p = \frac{P_{rated}}{0.5A\rho V_w^3} \tag{6}$$

The value of pitch angle is obtained by solving the nonlinear equation (2) using genetic algorithm (GA) based on (4), (5) and (6) which will be explained in the next sections.

III. GEAR RATIO CALCULATION

Here, A gearbox is necessary to adapt the low speed of the turbine rotor to the high speed of the generator. The gearbox conversion ratio (R_{GB}), also

known as the gear ratio, is designed to match the high-speed generator with the low-speed turbine blades. The gearbox ratio can be determined as follows:

- 1) Firstly, it is necessary to get the values of $C_{p,max}$ and λ_{opt} for gearbox ratio calculation. The values of $C_{p,max}$ and λ_{opt} in this work are 0.48 and 8.1, respectively.
- 2) Then, by using (1) at $C_{p,max}$, $V_w = 12m/sec$ and the rated value of wind turbine generator power which in this work is 1.5 MW. The blade length $R=30.6567m$ is easily found.
- 3) Then, it is necessary to get the value of rated turbine speed $w_{t-rated}$ which is calculated by using (5) at $V_w = 12m/sec$ and $\lambda = \lambda_{opt}$. The value of $w_{t-rated}$ in this work is $3.1706rad/sec$.
- 4) Finally, for a given rated speed of the generator and turbine, it is easily to calculate the gearbox ratio using (7) at rated value of generator speed which is equal to 1750 rpm and $w_{t-rated} = 30.277 rpm$ in this work. The value of gearbox ratio R_{GB} in this work is 57.7996.

$$R_{GB} = \frac{\text{generator rated speed in rpm.}}{\text{turbine rated speed in rpm.}} \quad (7)$$

The next figure shows the wind turbine equations with using the gear ratio as shown in Fig. 3.

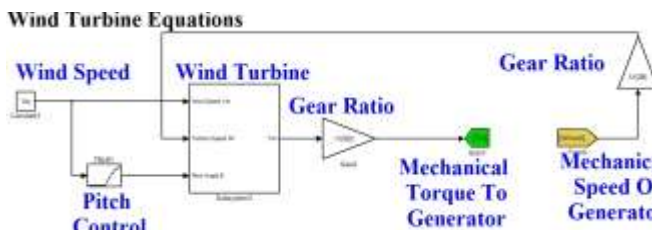


Fig. 3 Block diagram of wind turbine and the gear ratio in Matlab/Simulink.

The pitch control operation block shown in Fig. 3 will be explained in the next sections.

IV. GENETIC ALGORITHM OPTMIZATION

A. Principles of Genetic Algorithm

A genetic algorithm (GA) is a robust optimization technique based on natural selection [8-11].The basic goal of GA is to optimize functions called fitness functions. GA-based approaches differ from conventional problem- solving methods in several ways. First, GA works with a coding of the parameter set rather than the parameters themselves. Second, GA search from a population of points rather than a single point. Third, GA use payoff objective function information, not other auxiliary knowledge. Finally, GA use probabilistic transition rules, not deterministic rules. These properties make GA robust, powerful, and data-independent. A simple GA starts with a population of solutions encoded in one of many ways.

Binary encodings are quite common and are used in this report. The GA determines each string's strength based on an objective function and performs one or more of three genetic operators on certain strings in the population. GA concepts could be adapted into the form that is suitable for computer implementation. Fig.4 shows the flowchart of GA.

- 1) The Initialization generates an initial random population consisting of individuals whose characteristics are coded by the string of zeros and ones (Encoding the variables into binary strings).
- 2) The Elitism given a fitness function based on a suitable performance criterion; calculate a fitness value for each string within the population (Evaluation).
- 3) The Reproduction based on a probability basis; choose pairs of individuals to breed offspring strings, where individuals with a higher fitness value will be selected than those with a lower fitness value (Best fitness).
- 4) The Crossover divides the binary coding of each parent into two or more segments and then combines to give a new offspring string that has inherited part of its coding from each parent (The crossover used here is one cut point method).
- 5) The Mutation inverse bits in coding of the offspring with a low probability.
- 6) If search goal is achieved, or an allowable generation is attained, stop. Otherwise return to step (2).

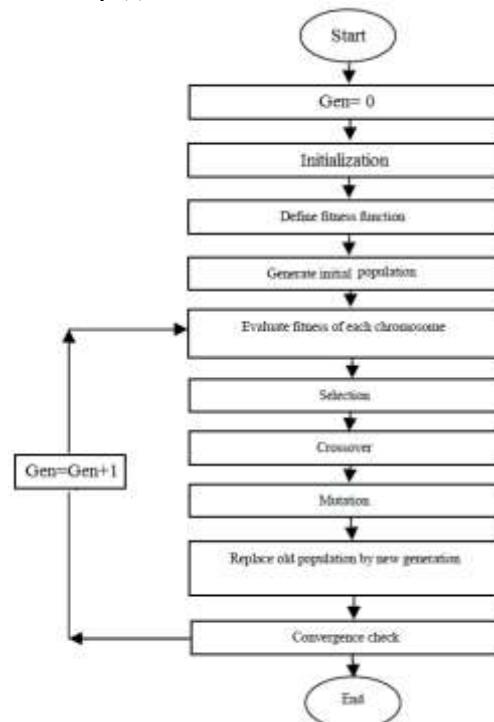


Fig. 4 The flowchart of GA.

B. Genetic Algorithm Controller for Pitch Control Mode

The genetic algorithm controller is used for getting the required value of pitch angle for each wind speed above the rated value to limit the output power and to protect the wind turbine from high wind speed in the region between the rated wind speed and cut out speed. As mentioned before to solve a nonlinear equation, it is preferable to use techniques such as GA. So, the following conditions must be taken into considerations in solving a nonlinear equation:

- 1) The power is at rated value P_{rated} from $V_w = 12 - 24m/sec$. The value of P_{rated} is 1.5 Mega watt.
- 2) The turbine speed is at rated value w_{t_rated} from $V_w = 12 - 24m/sec$. The value of $w_{t_rated} = 3.1706rad/sec$.

It is necessary to get the object function and define the required constrains. The equation used here is one variable equation. Then it is very important to know the constrains of the variable and the other parameters of genetic algorithm as the following [12]:

$$0 < \beta < 30$$

Where $\beta_{min} = 0$ and $\beta_{max} = 30$. The parameters used here for genetic algorithm are given in Table 1.

Table 1

Parameters of GA

Genetic Algorithm property	Value
Chromosome Length	16
Population Size	200
No. of iterations (Generations)	150

The object function used here is given as in (8):

$$Function = 0.5176 \left(\frac{116}{\lambda_i} - 0.4\beta - 5 \right) e^{-\frac{21}{\lambda_i}} + 0.0068\lambda - C_p = 0 \tag{8}$$

Where $\frac{1}{\lambda_i} = \frac{1}{\lambda + 0.08\beta} - \frac{0.035}{\beta^3 + 1}$ at $\lambda = \frac{w_{t_rated} R}{V_w}$ and $C_p = \frac{P_{rated}}{0.5A\rho V_w^3}$

Then, the above equation is solved by genetic algorithm under mentioned conditions. The result value of pitch angle obtained at $V_w = 15 m/sec$ (as a example for getting the value of pitch angle) after number of generations (Iterations) is shown in Fig. 5 using genetic algorithm GA. The pitch angle is obtained with changing the wind speed as shown in Fig. 6. As the wind speed increases more than rated wind speed, pitch control should be activated so as to limit the wind turbine from getting overload. When the pitch angle increases, C_p decreases and so does the tip speed ratio λ as shown in Fig. 7 and Fig. 8, respectively. Fig. 6 is modeled in equation using curve fitting algorithm in Matlab package as given in (9) and Fig. 9.

$$\beta(V_w) = p_1 V_w^4 + p_2 V_w^3 + p_3 V_w^2 + p_4 V_w^1 + p_5 \tag{9}$$

Where p_1, p_2, p_3, p_4 and p_5 are the coefficients and the range of V_w is $12 < V_w \leq 24$.

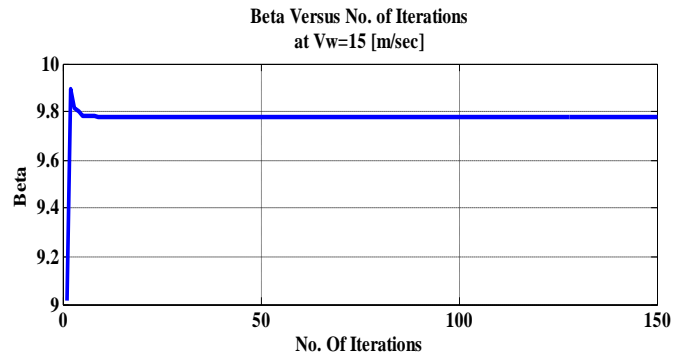


Fig. 5 Pitch angle β versus number of iterations.

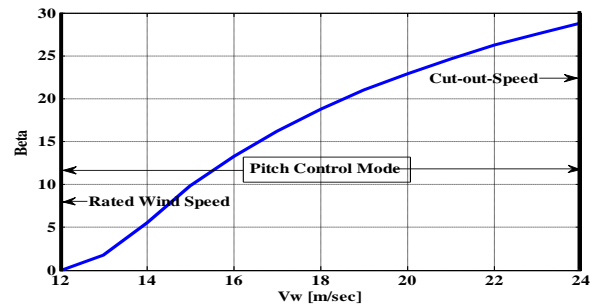


Fig. 6 Pitch angle β for various wind speeds in a variable-speed variable-pitch wind turbine system.

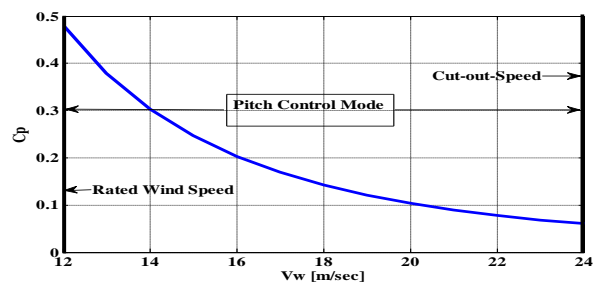


Fig. 7 The power coefficient C_p versus wind speed.

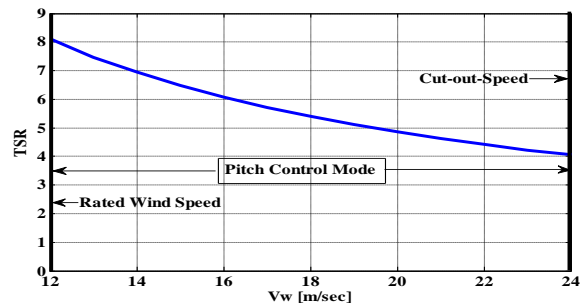


Fig. 8 TSR (λ) versus wind speed.



Fig. 9 Pitch angle β Vs wind speed V_w as a block in Mat lab/Simulink..

The wind turbine parameters used here in this paper is shown in Table 2.

Table 2

Parameters of Wind Turbine

Parameter	Symbol	Value and Units
Air density	ρ	1.225 Kg/m ³
Rotor radius	R	30.6567 m
Number of blades	$N_{p,blades}$	3
Rated wind speed	$V_{w,rated}$	12 m/sec
Cut-in/out wind speed	$V_{w,cut-in}/V_{w,cut-out}$	4/25 m/sec
Max C_p (MPPT)	$C_{p,max}$	0.48
Optimal λ (MPPT)	λ_{opt}	8.1
Rated Power	P_{rated}	1.5MW
Max/min pitch angle	β_{min}/β_{max}	30/0 degree
Gearbox Ratio	$R_{g,n}$	57.7996

V. DFIG MODEL

The DFIG-based WECS is shown in Fig. 10.

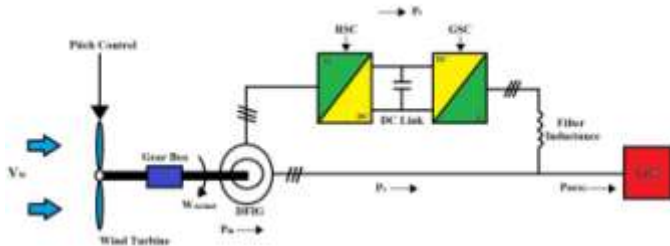


Fig. 10 DFIG based WECS

The dynamics of the DFIG is represented by a fourth-order state space model using the synchronously rotating reference frame (qd-frame) as given in (10)-(13) [13]:

$$V_{qs} = R_s I_{qs} + \omega_e \lambda_{ds} + \frac{d}{dt} \lambda_{qs} \quad (10)$$

$$V_{ds} = R_s I_{ds} - \omega_e \lambda_{qs} + \frac{d}{dt} \lambda_{ds} \quad (11)$$

$$V_{qr} = R_r I_{qr} + (\omega_e - \omega_r) \lambda_{dr} + \frac{d}{dt} \lambda_{qr} \quad (12)$$

$$V_{dr} = R_r I_{dr} - (\omega_e - \omega_r) \lambda_{qr} + \frac{d}{dt} \lambda_{dr} \quad (13)$$

Where V_{qs} , V_{ds} , V_{qr} and V_{dr} are the q and d-axis stator and rotor voltages, respectively. I_{qs} , I_{ds} , I_{qr} and I_{dr} are the q and d-axis stator and rotor currents, respectively. λ_{qs} , λ_{ds} , λ_{qr} and λ_{dr} are the q and d-axis stator and rotor fluxes, respectively. ω_e is the angular velocity of the synchronously rotating reference frame. ω_r is the rotor electrical angular speed. R_s and R_r are the stator and rotor resistances, respectively. The flux linkage equations are given as in (14)-(17):

$$\lambda_{qs} = L_s I_{qs} + L_m I_{qr} \quad (14)$$

$$\lambda_{ds} = L_s I_{ds} + L_m I_{dr} \quad (15)$$

$$\lambda_{qr} = L_r I_{qr} + L_m I_{qs} \quad (16)$$

$$\lambda_{dr} = L_r I_{dr} + L_m I_{ds} \quad (17)$$

Where L_s , L_r and L_m are the stator, rotor, and mutual inductances, respectively, with $L_s = L_{ls} + L_m$ and $L_r = L_{lr} + L_m$; L_{ls} and L_{lr} are the stator and rotor self inductance, respectively.

All the equations above are induction motor equations. When the induction motor operates as a generator, current direction will be opposite. The active and reactive power outputs from stator and rotor side are given as in (18)-(21):

$$P_s = \frac{3}{2} (V_{qs} I_{qs} + V_{ds} I_{ds}) \quad (18)$$

$$Q_s = \frac{3}{2} (V_{qs} I_{ds} - V_{ds} I_{qs}) \quad (19)$$

$$P_r = \frac{3}{2} (V_{qr} I_{qr} + V_{dr} I_{dr}) \quad (20)$$

$$Q_r = \frac{3}{2} (V_{qr} I_{dr} - V_{dr} I_{qr}) \quad (21)$$

The total active and reactive power generated by DFIG are given as in (22)-(23):

$$P_{total} = P_s + P_r \quad (22)$$

$$Q_{total} = Q_s + Q_r \quad (23)$$

If Total P_{total} and/or Total Q_{total} is negative, DFIG is supplying power to the power grid, else it is drawing power from the grid.

The electromagnetic torque T_e generated by the machine which can be written in terms of flux linkages and currents is given as in (24):

$$T_e = \frac{3 \cdot P}{2} (\lambda_{ds} I_{qs} - \lambda_{qs} I_{ds}) \quad (24)$$

Where P is the number of the pole pairs.

VI CONTROL OF DFIG WECS FOR PITCH CONTROLLER

Control of the DFIG is achieved by control of the variable frequency converter, which includes control of the RSC and control of the GSC as the following:

A. Design of the Rotor Side Converter RSC Controller

In DFIG wind energy systems, the stator of the generator is directly connected to the grid, and its voltage and frequency can be considered constant under the normal operating conditions. It is therefore, convenient to use stator voltage oriented control (SVOC) for the DFIG [14]. The stator voltage oriented control is achieved by aligning the d-axis of the synchronous reference frame with the stator voltage vector V_s . The resultant d- and q-axis stator voltages are: $V_{qs} = 0$ and $V_{ds} = V_s$. This DFIG control scheme is a rotor side control scheme where the stator reactive power is controlled by the direct current axis loop and the active power is controlled by the quadrature current axis loop. In the active power control loop the rotor electrical angular speed is compared with the

reference rotor electrical angular speed which is constant at its rated value for pitch controller and the error is fed to a conventional PI (Speed Regulator) controller to generate the reference quadrature axis current. Similarly, the stator side reactive power is calculated and is compared with the reference stator reactive power ($Q_{s,ref} = 0$) and the error is fed to another PI (Var Regulator) controller to generate the reference direct axis current. Then, both the direct and quadrature axis reference currents are converted from d-q axis reference frame to a-b-c frame. The three phase reference currents are compared with three phase rotor actual currents and the error is the input to hysteresis current controller and the output of this controller is the switch control signal to the firing gates of RSC. The band widths of the controllers are set at 5% of the rated current values. The hysteresis controller output gives the PWM switching pulses for the rotor side bidirectional converter control as shown in Fig. 11. The whole control scheme is simulated using Matlab/Simulink as shown in Fig. 12. The stator voltage vector angle θ_s is measured as shown in Fig. 13 and the rotor position angle θ_r is measured by an encoder mounted on the shaft of the generator. The slip angle θ_{sl} for the reference frame transformation can be obtained as the following ($\theta_{sl} = \theta_s - \theta_r$) as shown in Fig. 13.

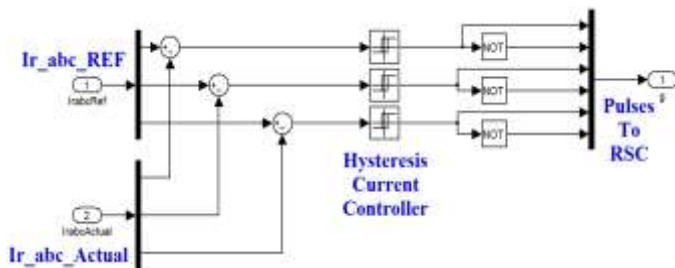


Fig. 11 Hysteresis current controller in Matlab/Simulink..

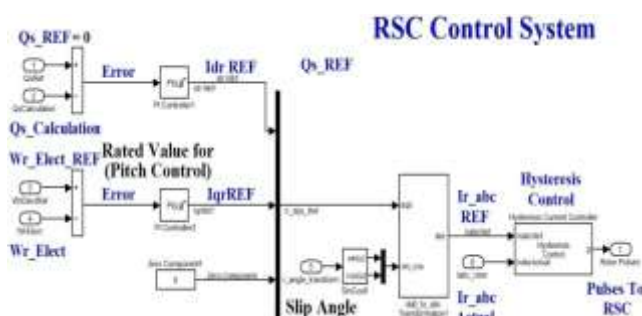


Fig. 12 Block diagram of RSC in Matlab/Simulink.

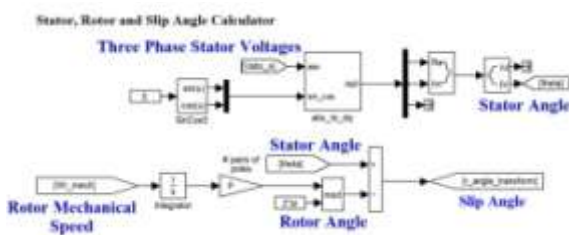


Fig. 13 Block diagram of stator, rotor and slip angle calculator in Matlab/Simulink..

B. Design of the Grid Side Converter GSC Controller

The goal of the control system of GSC is to maintain the DC-bus voltage constant at the required level for RSC, while the main input currents should be sinusoidal and in phase with their counterparts voltages, for which the control system of DFIG maintains unity power factor condition. The proposed control algorithm of GSC adopts the SVO technique to regulate DC-link voltage and achieve a unity power factor. This strategy leads to get and control the following active and reactive component fed to grid. This DFIG control scheme allows controlling the DC-bus voltage which is controlled by the direct current axis loop and the quadrature current axis which is kept at zero for unity power factor. The actual DC-bus voltage is compared with the reference DC-bus voltage and the error is fed to a conventional PI (DC Voltage Regulator) controller to generate the reference direct axis current. Then, the direct axis reference current of GSC is compared to the actual direct axis current of GSC and the error is fed to another conventional PI (Current Regulator) controller and the output of PI controller is control signal of direct axis voltage of GSC. Similarly, the quadrature axis reference current of GSC is compared to the actual quadrature axis current of GSC and the error is fed to another conventional PI (Current Regulator) controller and the output of PI controller is control signal of quadrature axis voltage of GSC. Then, the control signal of both direct and quadrature axis voltage are the input to PWM controller (Space Vector Modulator) and the output of this controller is the switch control signals (Pulses) to the firing gates of the GSC as shown in Fig. 14.

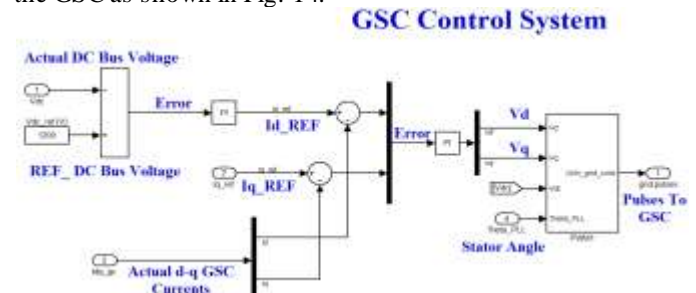


Fig. 14 Block diagram of GSC in Matlab/Simulink.

C. PI Controller Design

The output signal of a PI controller can be obtained as in (25):

$$U = K_p * e + K_i \int e * dt \tag{25}$$

Where e is the error signal, K_p and K_i are the proportional gain and integral gain, respectively. Choosing the appropriate control parameters of RSC and GSC is very important to gain good performance although the whole system might be able to work for a wide range of parameters. The most important objective is to maintain the system stability by selecting appropriate control parameters. And then

those parameters can be tuned up corresponding to the specified performance requirement. There are some methods that can be used to determine the system parameters that can keep the whole system in the stable region. One of the methods is by using Butterworth polynomial to optimize the closed loop eigen value locations [15]. The Butterworth method locates the eigen values uniformly in the left-half s-plane on a circle with radius ω_o , with its center at the origin as shown in Fig. 15.

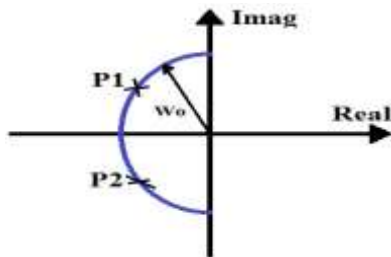


Fig. 15 Location of poles for second order Butterworth polynomial.

The Butterworth polynomial for a transfer function with a second order denominator is given as in (26):

$$p^2 + \sqrt{2} * \omega_o * p + \omega_o^2 = 0 \tag{26}$$

Where $p = \frac{d}{dt}$. The PI parameters are determined by comparing the coefficients in (26) with the denominators of the corresponding transfer functions and then choosing appropriate ω_o . Where ω_o is the bandwidth of the controller, which depends upon the design value. The system used has a significant advantage for the protection of the DFIG. It can naturally protect the system from over-current since current limiters can be easily inserted in the control system as shown in Fig. 12 and Fig. 14. The values of the parameters of each controller used in modeling of DFIG is shown in Table 3.

Table 3

Parameters of PI Controllers

ω_o		628 rad/sec	
RSC	Speed Regulator	k_{v,ω_r}	17.7715
		k_{r,ω_r}	7.8957
	Var Regulator	k_{v,ω_r}	$5.7798 * 10^{-4}$
		k_{r,ω_r}	0.0026
GSC	DC Voltage Regulator	$k_{v,v_{dc}}$	79.9719
		$k_{r,v_{dc}}$	3553.1
	Current Regulator	$k_{v,i}$	0.8846
		$k_{r,i}$	394.7842

VII RESULTS OF PITCH CONTROL USING GENETIC ALGORITHM CONTROLLER

The DFIG control structure is modeled and simulated in Matlab/Simulink and the overall model is shown in Fig. 16. The simulation is carried out under different conditions as the following:

- 1) Step change in wind speed.
- 2) Changing the value of generator inertia.

A. Effect of Changing Wind Speed

The simulation is carried out for a 1.5 MW DFIG-based WECS to verify the effectiveness of above described control system under varying wind speed. The DFIG parameters are shown in Table 4. The wind speed varies as shown in Fig. 17. When the wind speed is more than rated speed ($V_w = 12 \text{ m/sec}$), the wind turbine is operating in pitch control mode so $C_p < 0.48$ and $\lambda < 8.1$ with $\beta > 0$. Fig. 18, Fig. 19 and Fig. 20 show the time response of C_p , λ and β due to wind speed variation, respectively. When the wind speed varies, the rotor speed, the mechanical torque and mechanical power of generator response are kept constant at its rated as shown in Fig. 21, Fig 22 and Fig. 23, respectively. The stator, rotor and total active power output response of DFIG are kept limited each at its rated accordingly as shown in Fig. 24, Fig. 25 and Fig. 26 but the stator reactive power response is always regulated to zero as shown in Fig. 27 and achievement of unity power factor operation for both RSC and GSC as shown in Fig. 27 and 28, respectively. By doing so, the power factor of the overall DFIG wind turbine system can be regulated according to the requirement as shown in Fig. 29. During the entire operation period of the wind turbine, GSC maintains the DC-link voltage response in back to back converter of the DFIG to a constant value as shown in Fig. 30.

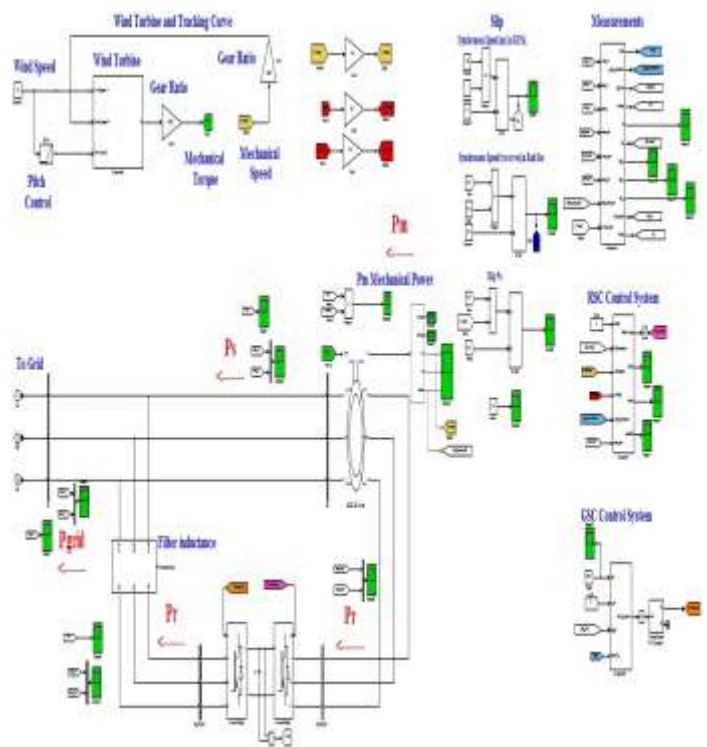


Fig. 16 Overall model of DFIG with pitch control in Matlab/Simulink.

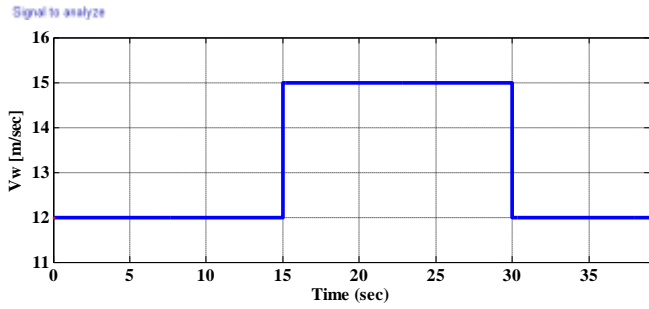


Fig. 17 Step change wind speed in Mat lab/Simulink.

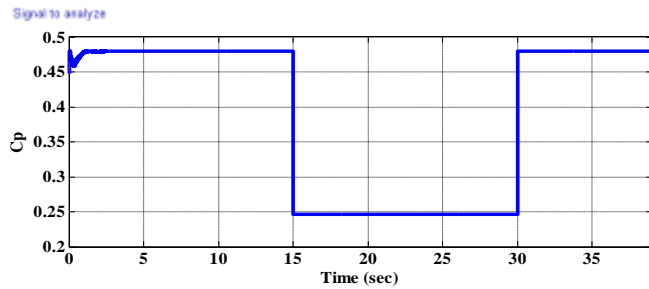


Fig. 18 Power coefficient C_p response during the variation of wind speed in Mat lab/Simulink.

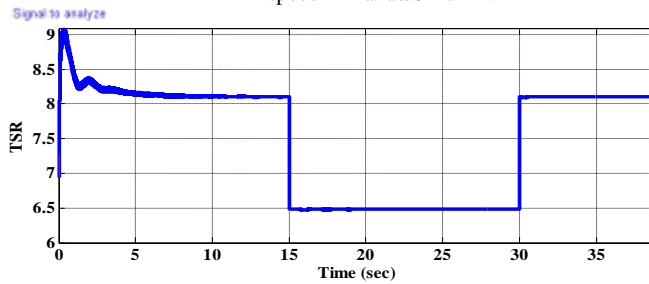


Fig. 19 Tip speed ratio λ response during the variation of wind speed in Mat lab/Simulink.

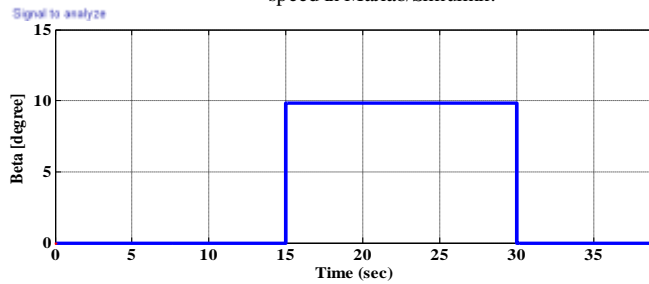


Fig. 20 Pitch Angle β response during the variation of wind speed in Mat lab/Simulink.

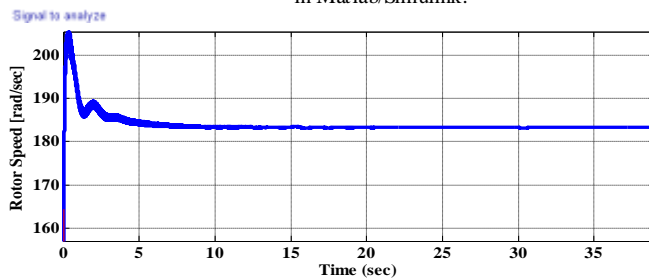


Fig. 21 Rotor speed of generator response during the variation of wind speed in Mat lab/Simulink.

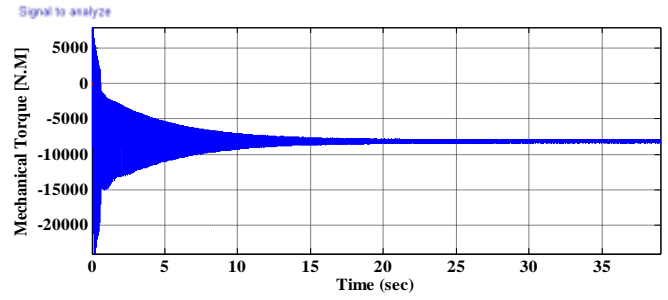


Fig. 22 Mechanical torque of generator response during the variation of wind speed in Mat lab/Simulink.

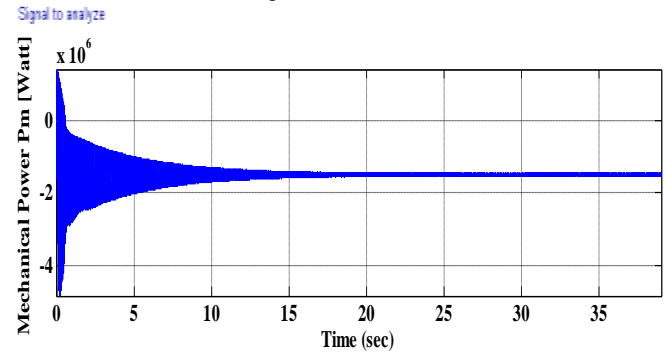


Fig. 23 Mechanical power of generator response during the variation of wind speed in Mat lab/Simulink.

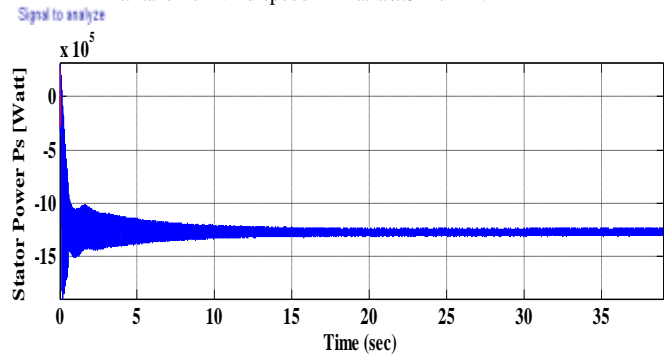


Fig. 24 Stator power of generator response during the variation of wind speed in Mat lab/Simulink.

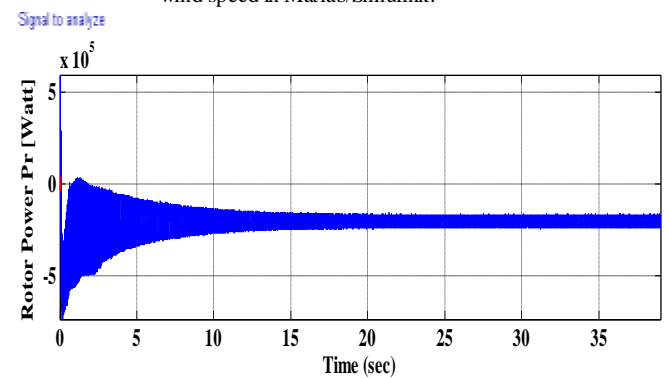


Fig. 25 Rotor power of generator response during the variation of wind speed in Mat lab/Simulink.

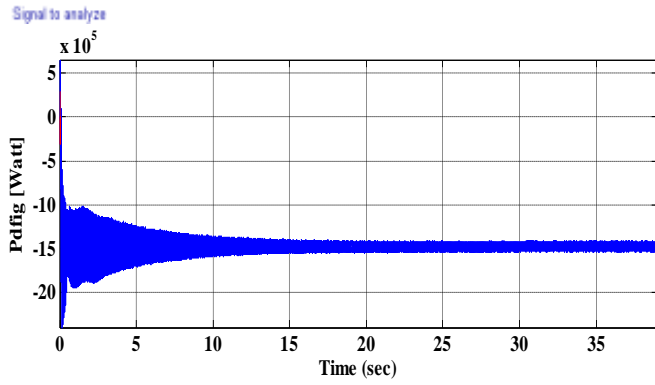


Fig. 26 Total active power response generated by DFIG during the variation of wind speed in Mat lab/Simulink.

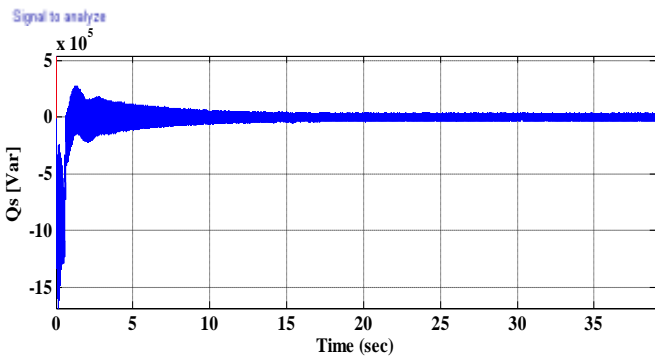


Fig. 27 Regulation of reactive power response during the variation of wind speed in Mat lab/Simulink.

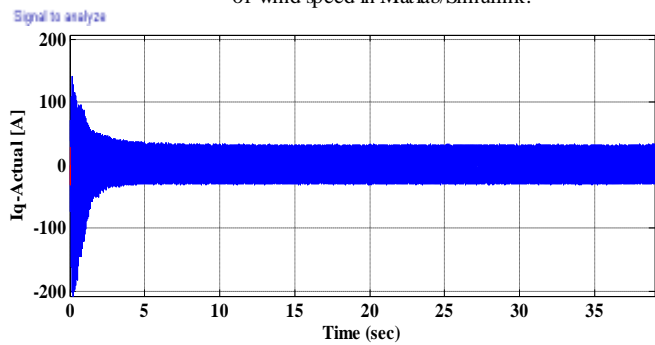


Fig. 28 The quadrature current axis response responsible for unity power factor during the variation of wind speed in Mat lab/Simulink.

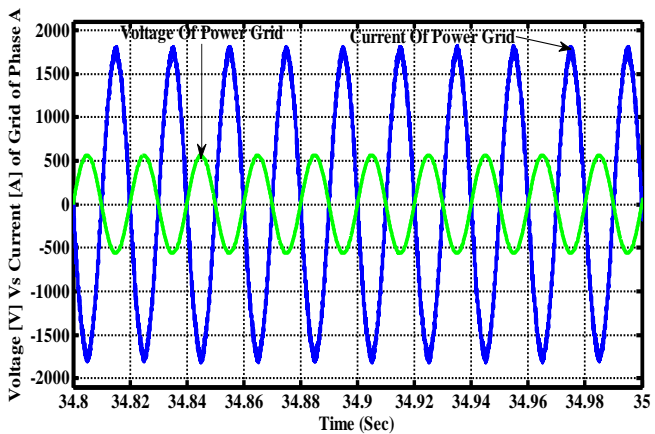


Fig. 29 Unity power factor by using DFIG for phase A.

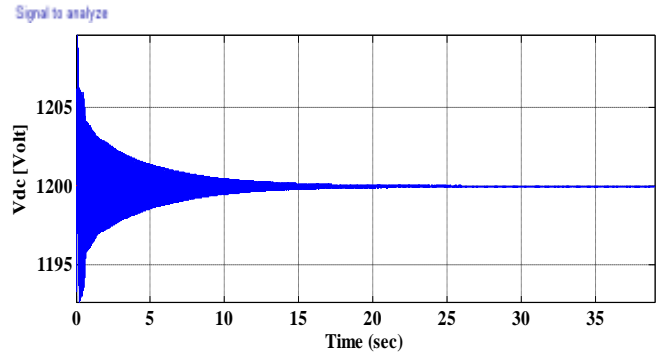


Fig. 30 The DC link voltage response during the variation of wind speed in Mat lab/Simulink.

Table 4

DFIG Parameters

Rated Mechanical Power	1.5 MW
Rated Stator Line-to-line Voltage	690 V (rms)
Rated Stator Frequency	50 Hz
Rated Rotor Speed	1750 rpm
Number of Pole Pairs	2
Rated Mechanical Torque	8.185 kN-m
Stator Winding Resistance, Rs	2.65 mΩ
Rotor Winding Resistance, Rr	2.63 mΩ
Stator Leakage Inductance, L _s	0.1687 mH
Rotor Leakage Inductance, L _r	0.1337 mH
Magnetizing Inductance, L _m	5.4749 mH
Shaft inertia	20 Kg.m ²
DC link voltage	1200 V
DC link capacitor	90 mF

B. Effect of Changing Inertia of Generator

For the same wind speed as mentioned above the system is studied and simulated for two values of generator inertia in order to indicate the effect of changing generator inertia on pitch control mode by displaying the next figures for power coefficient C_p and tip speed ratio λ . The first case for generator inertia $J = 40 \text{ Kg.m}^2$, the system is simulated and the results of C_p and λ response are shown in Fig. 31 and 32, respectively.

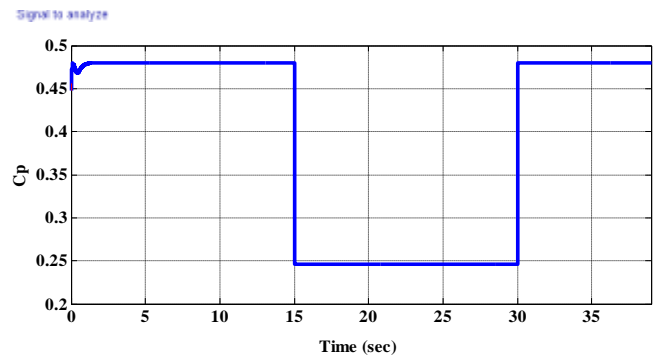


Fig. 31 Power coefficient C_p response during the changing of generator inertia $J = 40 \text{ Kg.m}^2$ in Mat lab/Simulink.

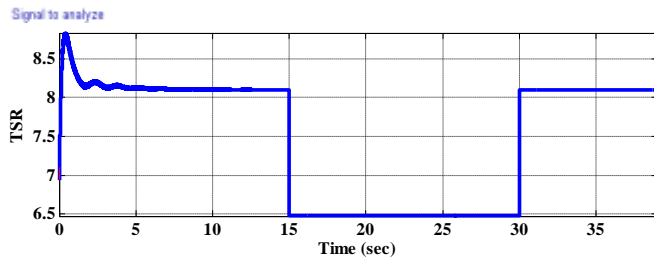


Fig. 32 Tip speed ratio λ response during the changing of generator inertia $J = 40 \text{ Kg.m}^2$ in Matlab/Simulink.

The second case for generator inertia $J = 15 \text{ Kg.m}^2$, the system is simulated and the results of C_p and λ response are shown in Fig. 33 and 34, respectively.

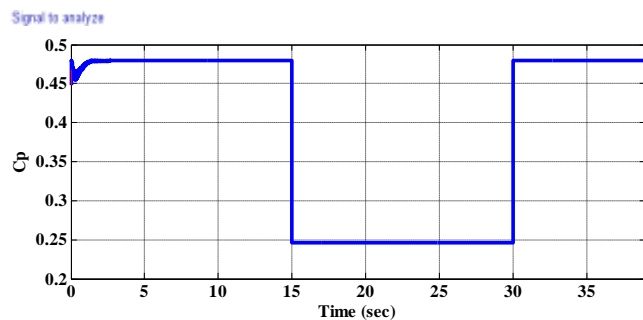


Fig. 33 Power coefficient C_p response during the changing of generator inertia $J = 15 \text{ Kg.m}^2$ in Matlab/Simulink.

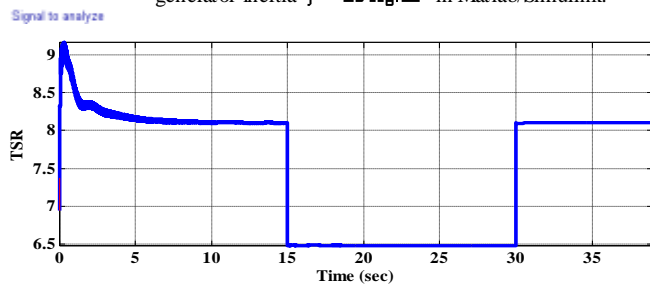


Fig. 34 Tip speed ratio λ response during the changing of generator inertia $J = 15 \text{ Kg.m}^2$ in Matlab/Simulink.

The results displayed above show that the DFIG has the ability to keep the power limited at its rated (Constant value) at different values of generator inertia for step change in wind speed.

VIII. CONCLUSIONS

The genetic algorithm is used to design pitch angle controller to limit the wind turbine mechanical power at rated value under wind speed over rated value operation. The above region of WECS is called constant power operation. The DFIG with two control algorithm called GSC and RSC. The stator voltage orientation (SVO) control algorithms is utilized for RSC which is controlled by hysteresis current controller. While the GSC is controlled by pulse width modulation (PWM). The model of DFIG is described and simulated in Matlab/Simulink package. The PI controllers are designed for DC voltage control and active and reactive power control of RSC and

GSC control system of DFIG . The effect of wind speed variation above rated value using the genetic pitch angle control in terms of generator rotor speed, mechanical power, mechanical torque, stator power , rotor power responses. The proposed PI controllers can achieve unity power factor at grid side. Also, the effect of generator inertia variations is studied. The digital results show the effectiveness and powerful of the genetic pitch angle control in sense of fast responses of generator states due to wind speed variations.

REFERENCES

- [1] M Anju and R Rajasekaran. "Co-Ordination Of SMES With STATCOM For Mitigating SSR And Damping Power System Oscillations In A Series Compensated Wind Power System". IEEE 2013 International Conference on Computer Communication and Informatics (ICCCI -2013), 2013.
- [2] J Morren and SWH de Haan. "Ride through of wind turbines with doubly-fed induction generator during a voltage dip". IEEE Transaction. Energy Converters. 2005; 20(2): 707–710.
- [3] DNV/Risø, "Guidelines for design of wind turbines", 2nd ed., Jydsk Centraltrykkeri, Denmark, 2002.
- [4] S. Suryanarayanan, A. Dixit, "Control of large wind turbines: Review and suggested approach to multivariable design", Proc. Of the American Control Conference 2005,Portland, USA, pp. 686-690.
- [5] Grisales, L. T., Lemus, C. to sp G., and Sergio, S., "Overall Description of Wind Power Systems", in ing. Ciencenero-junio., Vol. 10, pp. 99–126,2014.
- [6] Thongam, J. S. and Ouhrouche, M. , "MPPT Control Methods in Wind Energy Conversion Systems", in Intech open, Vol 15, pp. 339-360, June 2011.
- [7] Zhe, C., et al., "A Review of the State of the Art of Power Electronics for Wind Turbines," IEEE Transactions on Power Electronics, Vol. 24, pp. 1859-1875, 2009.
- [8] Salami, M., Cain, G., "The Quest for a New Computing Architecture Based on Genetic Algorithms", Proceedings of the Electrical Engineering Congress (EEC94) , Sydney, Australia, November 1994.
- [9] Abdullah, M. A., Yatim, H. M. and Tan,C. W., "Particle Swarm Optimization-Based Maximum Power Point Tracking Algorithm for Wind Energy Conversion System, "in IEEE International Conference on Power and Energy (PECon), pp.978-1-4673-5019, December 2012.
- [10] [Chen, J. H. , Yau, H. T. , and Hung, W. , "Design and Study on Sliding Mode Extremum Seeking Control of the Chaos Embedded Particle Swarm Optimization for Maximum Power Point Tracking in Wind Power Systems", in MDPI , Vol 7, pp. 1706-1720, March 2014.
- [11] B. Vasumathi, S. Moorthi, " Harmonic Estimation Using Modified ADALINE Algorithm with Time-Variant Widrow-Hoff (TVWH) Learning Rule", Computers & Informatics (ISCI), 2011 IEEE Symposium, 2011, pp.113-118.
- [12] Endusa Billy Muhandu, Tomonobu Senju, Aki Uehara, Toshihisa Funabashi, and Chul-Hwan Kim, "LQG Design for Megawatt-Class WECS With DFIG Based on Functional Models' Fidelity Prerequisites," IEEE Trans. on Energy Conversion, vol. 24, no. 4, pp. 893-904, Dec. 2009.
- [13] Krause, O. Wasynczuk, and S. D. Sudhoff, Analysis of Electric Machinery and Drive Systems, IEEE Press, Wiley-Inter science, John Wiley & Sons, Inc., New Jersey, 2002.
- [14] S. Müller, M. Deicke, and R. W. De Doncker, Doubly Fed Induction Generator Systems for Wind Turbines, IEEE Industry Applications Magazine, Vol. 8, No. 3, 26-33, 2.
- [15] Gan Dong, "Sensor less and Efficiency Optimized Induction Machine Control with Associated Converter PWM Modulation Schemes," Ph.D. dissertation, Tennessee Technological University, Dec. 2005.